

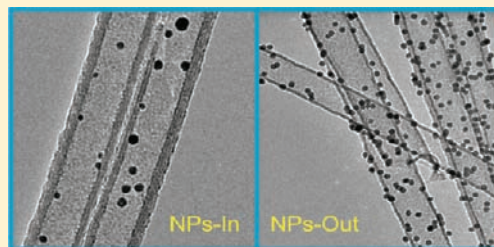
Wall-Selective Chemical Alteration of Silicon Nanotube Molecular Carriers

Moshit Ben-Ishai and Fernando Patolsky*

School of Chemistry, The Raymond and Beverly Sackler Faculty of Exact Sciences, Tel Aviv University, Tel Aviv 69978, Israel

S Supporting Information

ABSTRACT: Recently, there has been significant interest in the synthesis and potential applications of semiconductor nanotubes (NTs). In this context, many efforts have been invested in developing new routes to control and engineer their surface chemistry. We report herein on a simple route to differentially and selectively functionalize the inner and outer surfaces of silicon nanotubes (SiNTs) with organic molecular layers containing different functional groups and hydrophobicity/hydrophilicity chemical nature, via covalent binding, to give nanotubular structures with dual chemical properties. Significantly, our unique synthetic approach can be further extended to directly form hollow crystalline nanotubular structures with their inner/outer surfaces independently and selectively altered chemically. Additionally, SiNTs inner and/or outer walls can be selectively decorated with metal nanoparticles. Both inner and outer walls can be individually and separately modified with the same metal nanoparticles, with different metal NPs in the inside and outside walls or with a combination of metal NPs decoration and molecular layers, if so required. Furthermore, the dually modified nanotubes were then exploited as phase extraction nanocarriers to demonstrate their potential in future chemical and biological separation, extraction, and filtering applications.



INTRODUCTION

Among recent developments in new synthetic approaches of semiconductor nanotubes (NTs),^{1–14} there has been significant interest in their potential applications,^{7,15–23} with the motivation of creating new routes to independently and selectively control and engineer their surface chemistry.^{24–38} It has been recognized that engineering the surfaces of nanotubular structures with various functional groups may provide effective routes to tune, as well as to enhance, their surface properties (i.e., solubility, electronic properties), to better fit many unique and desirable applications, including selective transport,^{22,39–42} chemical separations (selective filtering), and sensing of chemical and biological molecules. Significantly, selective modification of the surfaces of nanotubular structures with various functional groups may lead to complex multifunctional nanostructures, while largely retaining their structural integrity. Although there have been much efforts to chemically modify both organic and inorganic nanotubes with various chemical functional groups,^{35,43–47} including covalent and noncovalent functionalization of the sidewalls, there are only two reports about selective modifications of the inner versus outer surfaces of amorphous insulating silica and titania nanotubes using nanopore alumina template membranes²³ and electro-spinning technique⁴⁸ respectively, and to our knowledge, no prior research on the controlled and systematic wall-selective modifications of semiconducting inorganic nanotubes has been reported. Silicon nanotubes (SiNTs) have recently attracted a considerable attention due to their technological future potential.^{49–51} In addition, their noncytotoxic nature makes them potential candidates for a large variety of biotechnological applications.

We report herein on a simple route to differentially and selectively functionalize the inner and outer surfaces of silicon nanotubes with organic molecular layers containing different functional groups and hydrophobicity/hydrophilicity chemical nature, via covalent binding, to give nanotubular structures with dual chemical properties. Our previous work on crystalline silicon and silicon–germanium alloy nanotubular structures⁵² shows several unique advantages that make these nanotubes potential candidates for chemical and biological applications. Significantly, our developed synthetic approach can be further extended to directly form hollow crystalline nanotubular structures with their inner/outer surfaces independently and selectively altered chemically. Additionally, SiNTs inner and/or outer walls can be selectively decorated with metal nanoparticles. Both inner and outer walls can be individually and separately modified with the same metal nanoparticles, with different metal NPs in the inside and outside walls or with a combination of metal NPs decoration and molecular layers, if so required. Furthermore, the dually modified nanotubes were then exploited as phase extraction nanocarriers to demonstrate their potential in future chemical and biological separation, extraction and filtering applications.

EXPERIMENTAL SECTION

Synthesis of Nanowires (MWs) Precursors. Core-multishell-nanowire heterostructures were synthesized by chemical vapor deposition

Received: October 24, 2010

Published: January 7, 2011

as previously described.^{52–54} Gold nanoparticles (Ted Pella) of a given diameter, which served as catalyst sites for the VLS-CVD growth of Ge nanowire cores, were initially deposited on Si(100) growth substrates. To promote the adhesion of the gold nanoparticles to the silicon substrate, a poly-L-lysine solution (Ted Pella) was applied to the bare silicon wafer, as an electrostatic binding agent. The nanoparticle-deposited wafer was then placed in a horizontal tube furnace for the growth of the Ge–Si core–shell NWS.^{52–54}

Nanotubes Surface Modification . Step I: Outer-Surface Modification Process. The modifications process of the exterior surface was carried out directly on the Ge–Si core–shell nanowire templates. The substrate-bound nanowires were incubated in various solutions of silanes derivatives for nearly 4 h to yield either hydrophilic or hydrophobic outer surface: 1% aminosilane in water and ethanol, 2% fluorosilane and 2% octadecylsilane in dichloromethane, and 5% mercaptosilane in ethanol.

The samples were then rinsed with an appropriate solvent and cured for 10 min at 110 °C. After sonication and Ge-etching steps, the resulting modified NTs were centrifuged and redispersed in an appropriate solvent. At this stage, the outer-wall modified SiNTs can be readily modified in their inner wall surfaces.

Step II: Inner-Surface Modification Process. The modified silicon nanotubes were dispersed in an appropriate solvent, depending on the outer-wall modification, and incubated with different silane derivatives to give either hydrophobic or hydrophilic inner surfaces. The following mixtures were shaken for 4 h: 5% octadecylsilane (or 5% fluorosilane) was added into ethanol suspensions of aminosilane-functionalized nanotubes; 2% aminosilane (or 5% fluorosilane) was added into dispersions of nanotubes modified with mercaptosilane in ethanol; 2% aminosilane (or 5% mercaptosilane) was added into suspensions of nanotubes modified with fluorosilane in dichloromethane; and 2% octadecylsilane was added into a dispersion of nanotubes functionalized with octadecylsilane in ethanol. Finally, the samples were centrifuged, washed, and redispersed in appropriate solvents.

Sample Characterization. XPS studies were performed on silicon wafers deposited with a thick film of the modified NTs, using 5600 Multi-Technique System (PHI) with a base pressure of 2.5×10^{-10} . The analysis chamber was equipped with a monochromated Al K α X-ray source ($h\nu = 1486.6$ eV) and spherical capacitor analyzer using slit aperture of 0.8 mm. Charge compensation was achieved (if required) by charge neutralizer. XPS data were referenced with respect to the C1s binding energy of 285 eV. All the detailed XPS spectra reported in this work are supported by published database.^{55–57}

Fluorescence spectra were recorded by a Perkin-Elmer LS55 luminescence spectrometer using an excitation wavelength of 488 nm.

Accurate TEM measurements of the dimensions and structural and morphological analysis of AuNPs-decorated SiNTs were performed using a High-Resolution Transmission Electron Microscope (FEG-HTEM, Technai F20). The solution of the NTs structures was deposited dropwise on lacy-carbon TEM grids for their morphological and structural analysis.

Selective Decoration of Gold Nanoparticles onto SiNTs. The gold/SiNT composites were prepared by an electroless deposition method comprising the following steps: First, the substrate-bound Si/Ge core–shell nanowires were immersed into a 12 mM HF (40% in water) solution for 5 s, to etch the native oxide layer, then rinsed with water and immediately immersed into a solution of 1 μ M KAuCl₄ and 12 mM HF (40%) in ethanol for 2 min to form Au nanoparticles. The sample was then rinsed with ethanol, followed by sonication of the gold decorated NWs in ethanol and etching of the Ge core with 1:3 (v/v) H₂O₂/ethanol at 60 °C for 2 h.

Selective Decoration of Gold Nanoparticles on SiNTs Inner-Wall. The substrate-bound Ge–Si core–shell nanowires were first “knocked down” by sliding the growth substrate onto bare silicon wafer, followed

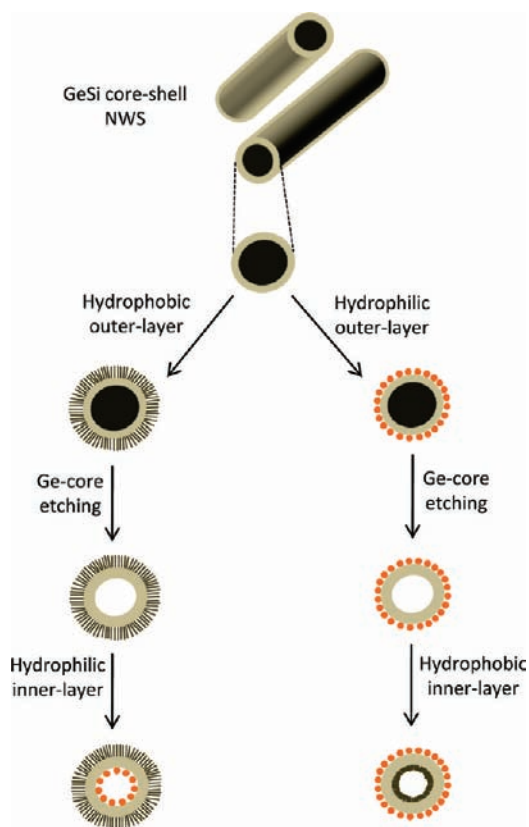


Figure 1. Schematics of the approach used for the wall-selective functionalization of the outer and inner surfaces of SiNTs by various silane-derivatives molecular layers.

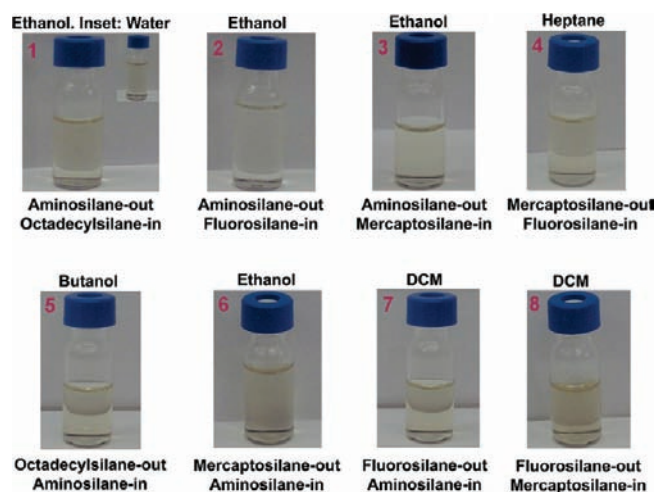
by chemical modification with fluorosilane molecules, and selective etching of the Ge core to form SiNTs (the “knock-down” step was performed in order to receive open-ended core–shell nanowires that will finally allow the chemical removal of Germanium cores when required).⁵⁸ The substrate-bound modified SiNTs were immersed into 12 mM HF (40%) in water for 3 min to etch the native oxide layer of the inner-walls, then rinsed with water and immersed into a solution of 1 μ M KAuCl₄ in ethanol for 40 min to form Au nanoparticles inside the SiNTs. The gold decorated NTs were centrifuged and washed several times with ethanol and deposited on lacy-carbon copper grid for TEM measurements.

RESULTS AND DISCUSSION

Our strategy for the wall-selective modification of SiNTs relies on our synthetic approach of silicon nanotubular structures, as described previously.⁵² Briefly, silicon nanotubular structures were prepared using Ge(core)–Si(shell) nanowire heterostructure templates via CVD-VLS method and transformed into hollow nanostructures by selective wet chemical etching of the germanium core. Figure 1 schematically describes our synthetic approach accompanied by the functionalization procedure that generates silicon nanotubes with independently and selectively modified inner and outer surfaces. In our present study, the modification process of nanotubes was carried out using silane derivatives with different functional groups, via wet chemistry procedures. The outer surface of the core–shell nanowire and the inner surface of the subsequent silicon nanotubes are terminated by silanol groups (SiOH), which are employed as anchoring sites for silane molecules to form Si–O–Si covalent bonds.^{55–57} The first step, outer surface modification, was

Table 1. Results of XPS Elemental Analysis in at. Percent (%) for Samples Described in Figure 2

element	ref	sample 1	sample 2	sample 3	sample 4	sample 5	sample 6	sample 7	sample 8
C	13.01	32.28	25.74	40.79	28.51	44.18	27.12	28.00	24.80
O	32.77	35.00	24.09	32.77	24.41	32.21	37.66	18.53	24.66
Si	51.66	30.07	16.68	14.76	20.08	16.36	24.45	12.48	24.67
N	-	2.45	2.22	4.02	-	5.51	3.04	1.92	-
S	-	-	-	5.97	3.64	-	4.21	-	1.13
F	-	-	31.28	-	-	-	0.49	39.07	24.75
Ge	2.56	0.21	-	-	-	0.20	-	-	-
Cl	-	-	-	-	-	-	-	-	-
P	-	-	-	1.79	-	-	2.35	-	-

**Figure 2.** Dispersions of the differentially functionalized SiNTs in various solvents.

carried out directly on the surface of the core–shell nanowire templates, by incubating the substrate-bound nanowires in a solution of a silane derivative for a period of 4 h. This allows us to selectively modify the external surface of the subsequent nanotubes without affecting their inner surface. The modified nanowire substrate was then rinsed with an appropriate solvent and cured for 10 min in an oven at 110 °C. The next step, which involves the removal of the outer-wall modified nanowires from the growth substrate by sonication and selective extraction of the germanium core, results in the formation of hollow silicon nanostructures with either hydrophobic or hydrophilic exterior surface depending on the nature of the first attached molecules. At this stage, the NTs' interior, which was left unfunctionalized, possesses a hydrophilic void. Prior to the internal modification process, the resultant functionalized nanotubes were centrifuged, washed, and dispersed into liquid suspensions. Next, the outer-wall modified nanotubes were subjected to a second chemical modification process on their inner wall surfaces. This was done by incubating the nanotubes suspensions with silane molecules possessing different functional groups from those attached to the outer surface. The mixture was slightly shaken for 4 h, centrifuged, washed, and dispersed in appropriate solvents. Table 1 summarizes all the chemical modifications performed on the surfaces of the silicon nanotubes. Representative results of the orthogonal functionalization of the silicon nanotubes are illustrated in Figure 2. It is worth pointing out that pristine silicon nanotubes are insoluble in most solvents and have strong tendency to form aggregates shortly after their removal from

the growth substrate by sonication (even in ethanol which is considered as a favorable solvent for the preparation of SiNWs suspensions). Stable suspensions of the silicon nanotubes in different solvents (common organic solvents and water) manifest successful modification of the outer surface of the nanotubes with molecular layers, which are well-known to facilitate solubility of both nanowires and nanotubes.

To characterize the surface state of the silicon nanotubes, we carried out X-ray Photoelectron Spectroscopy (XPS) analysis, before and after each performed functionalization step. Low-resolution XPS analysis, as shown in Figure 3, for the studied samples described in Figure 2, shows that the modification process induces significant changes in the sample elemental composition, in comparison with the reference SiNTs pristine sample (Figure 3A), and provides clear evidence that the silicon nanotubes have been chemically modified. The XPS elemental analysis of the as-received SiNTs reveals the presence of mainly silicon, oxygen, as well as trace amounts of carbon. The latter component can be attributed to adventitious carbon sources and also to traces of organic solvents involved in the wet-chemical etching process of the Ge cores. As a result, the void of the resultant nanotubes might contain residues of organic solvents, which are subsequently replaced by the silane molecules in the second chemical modification step of the inner NTs walls. Thus, in order to eliminate the contribution of carbon element residues coming from the wet etching process, we used the pristine core–shell nanowires sample as a reference system.

The XPS data of all the silanized NTs reveal additional spectral components. The XPS survey spectrum of the nanotubes modified by octadecylsilane and aminosilane layers (Figure 3B,F) reveals a signal at 400 eV which is assigned to amine groups and an intense peak of C12p at 200 eV which can be attributed to the alkyl chain of the octadecylsilane molecular layer. The XPS spectra obtained from samples 2 and 7 (Figure 3C,H) show an intense signal around 690 and at 400 eV corresponding to the F1s and N1s regions, respectively, both indicating the presence of fluorosilane (inner or outer) and aminosilane (inner or outer) molecular layers on the nanotube surfaces. The N1s and S2p peaks at 400 and at 228 eV, respectively, observed for samples 3 and 6 (Figure 3D,G) can be attributed to aminosilane and mercaptosilane molecular layers, and the S2p and F1s elements located at 228 and 690 eV detected for samples 4 and 8 (Figure 3E,I) indicate the presence of mercaptosilane and fluorosilane species on the NTs wall surfaces. The absence of the aforementioned components in the XPS spectra of the bare silicon nanotubes further manifests the successful modification process of the inner and outer walls of the nanotubular structures. Moreover, the results of XPS elemental analysis (Table 1)

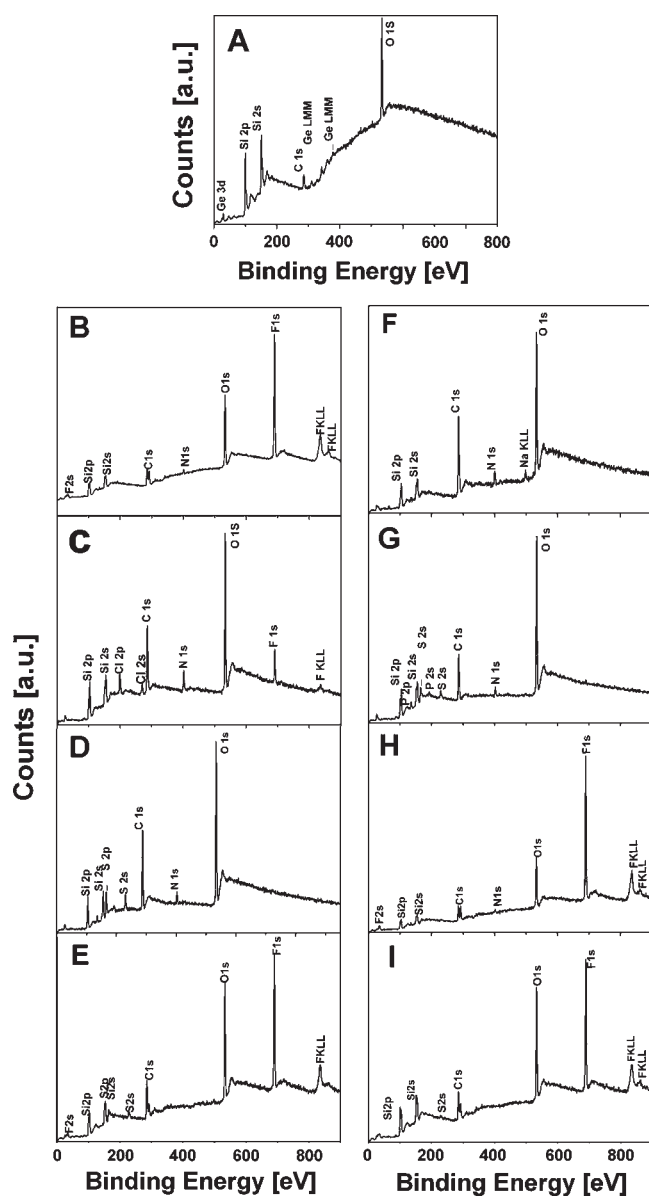


Figure 3. Set of representative X-ray photoelectron survey spectra of (A) Ge–Si core–shell nanowire reference sample; (B) sample 1; (C) sample 2; (D) sample 3; (E) sample 4; (F) sample 5; (G) sample 6; (H) sample 7; (I) sample 8.

obtained from the corresponding XPS spectra (Figure 3) show a clear enhancement in the atomic ratio of C/Si for the functionalized samples (1.6:1 in average) in comparison with that measured from the raw unmodified nanotubes sample (\sim 1:4). This observation provides additional support to the presence of the alkyl silane molecules on the surfaces of the nanotubes. Especially noteworthy is the increase in the average atomic ratio of C/Si, from 0.7 to 1.7, before and after the second modification step, respectively (data not shown). This result provides complementary indication for the successful creation of an alkyl silane molecular layer.

To rule out the possibility that the second modification step does not also occur on the already modified exterior NTs surface, and to further confirm the efficiency of the orthogonal surface modification process, we conducted control experiments, in which the modified core–shell nanowires were exposed to a

second modification step, prior to the etching process of the germanium cores. To that end, the substrate of octadecylsilane-modified core–shell nanowires was incubated in an aminosilane derivative ethanolic solution for a period of 4 h. After washing and curing, XPS analysis was applied to elucidate the surface state of these nanowires (see Supporting Information, Figure S1). The absence of a signal at 400 eV, which is ascribed to the presence of amine functional groups on the NTs surface, clearly indicates that aminosilane molecules cannot access the exterior surface of the core–shell nanowires after the first silanization step had occurred. The same phenomenon was also observed after treatment of aminosilane-modified core–shell nanowires with mercaptosilane molecules (see Supporting Information, Figure S2). Thus, no mixing of silane derivatives occurs on the surfaces of the SiNTs.

Detailed analysis of the XPS spectra provides clear evidence that the SiNTs were chemically modified. Figure 4 shows a set of representative high-resolution XPS spectra of the Si2p region of the pristine (Figure 4A) and the modified NTs samples. The silicon Si2p peak observed at 103 eV corresponding to the silicon oxide layer present in the pristine sample (Figure 4A) is shifted to lower binding energies with a higher value for the full width at a half-maximum (fwhm) following the performed chemical treatments. The silicon oxide Si2p peak in the modified samples can be decomposed into two contributing peaks appearing at around 103 eV and at 101.5 eV, as shown in Supporting Information Figure S3, for samples modified with aminosilane and octadecylsilane (samples 1 and 5). The component at 103 eV corresponds to silicon oxide and the later component, which does not appear in the pristine sample, can be attributed to either O–Si–C bond, coming from the silane molecules or to the silicon participant from the siloxane network (Si–O–Si) (marked with dashed pink line, or the pink peak in Figure S3), resulting from the condensation of silane molecules. Additionally, the Si2p component (marked with a red dashed line) located at 100 eV, not observed in the bare NTs sample, can be attributed to Si-bonded carbon originating from the alkyl chains of the surface-anchored silane molecules. These assignments together with the absence of the aforementioned signals in the pristine sample provide strong evidence for the incorporation of silane molecules to the surfaces of the silicon nanotubes.

Figure 5 shows a series of representative high-resolution XPS spectra of the carbon C1s region of the pre- and post-treated NTs samples. The carbon peak in the raw unmodified sample (Figure 5A) is the sum of C1s electrons from adventitious carbon sources. The lower energy peak at 285 eV can be ascribed to adventitious carbon bonded to either hydrogen or another carbon atom, and the higher binding energy peak at 286.6 eV can be ascribed to adventitious carbon bonded to oxygen. Following the silane treatment, new carbon species, which are components characteristic of the silane molecules, appear in the spectra of the modified samples, in addition to those obtained for the raw sample. Additionally, the peak at 285 eV which corresponds to C–H/C–C bonds, possess a higher value for the full width at a half-maximum (fwhm) and prominent “knee” at low binding energy of 284 eV which can be attributed to C–Si bond coming from the silane molecules. A detailed view of the carbon C1s spectrum of the samples modified with both mercaptosilane and fluorosilane molecules (samples 4 and 8) (Figure 5B) reveals two components at 293.2 and 291.1 eV, respectively, which are assigned to the CF₂ and CF₃ groups present on the fluorosilane, and two more new components at 285.5 eV, which is characteristic

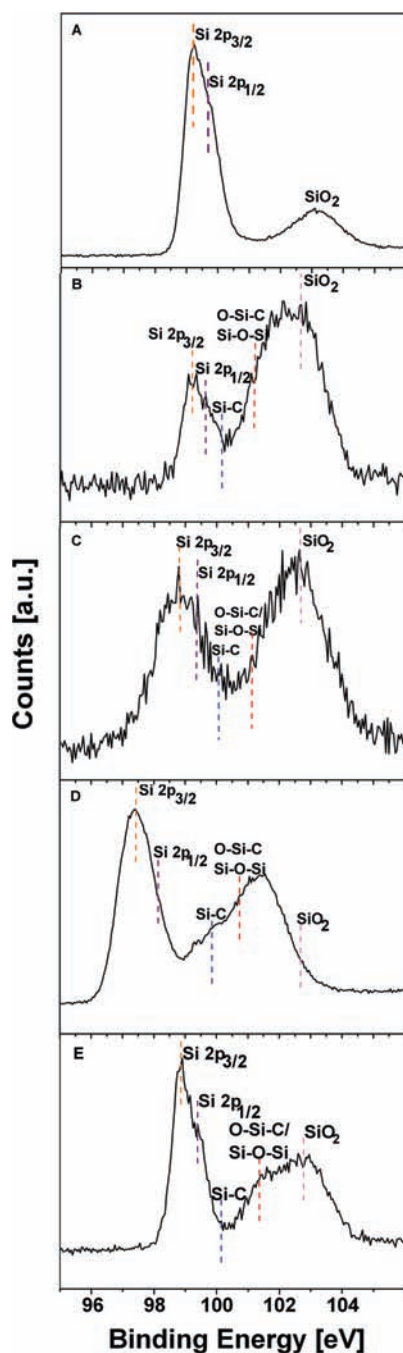


Figure 4. Series of representative high-resolution XPS spectra of the Si 2p region for: (A) core-shell nanowire reference sample, (B) samples modified with aminosilane molecules and octadecylsilane molecules (sample 1 and 5), (C) samples modified with aminosilane and fluorosilane molecules (sample 2 and 7), (D) samples modified with aminosilane and mercaptosilane molecules (sample 3 and 6), and (E) samples modified with mercaptosilane and fluorosilane molecules (sample 4 and 8) showing SiO₂ (pink dashed line), C–Si–O or Si–O–Si (brown dashed line), Si–C (blue dashed line), and Si 2p_{1/2} (purple dashed line) and Si 2p_{3/2} (orange dashed line).

of carbon bonded to thiol group, and at 284.0 eV which corresponds to C–Si bond, coming from the silane molecule. The presence of C–SH bond is also confirmed by the high-resolution XPS spectra of the S2s region, as will be shown later. The C1s characterized by binding energy of 286.6 eV is ascribed

to adventitious carbon bonded to oxygen from both the wet chemical modification processing and wet chemical etching of the germanium core. Figure 5C shows a representative spectrum of samples 2 and 7, which are both modified with fluorosilane and aminosilane molecules. In addition to the aforementioned components, the spectrum in Figure 5C reveals new species at 286 eV, which can be attributed to carbon-bonded nitrogen indicating the presence of aminosilane molecules on the surface of the nanotubes. This component was also observed in the C1s spectrum of samples 3 and 6 (Figure 5D), which were treated with aminosilane molecules on either the exterior or interior NTs surface, and also in the C1s spectrum of samples 1 and 5 (Figure 5E) which were derivatized with aminosilane and octadecylsilane molecules. Note, the C1s spectra of all modified samples reveal a component characteristic of C–Si, which is assigned to the silane molecular layer. To further elucidate the surface state of the modified samples and to acquire further evidence for the chemical modification of the silane species onto the NTs surfaces, high-resolution XPS analysis of N1s and S2s regions was also carried out. Representative N1s and S2s spectra are shown in Figures 6 and 7, respectively. It is observed that N1s spectrum (Figure 6) consists of two components: one component corresponding to amino groups at around 399 eV and another component corresponding to protonated amino groups at 401 eV, suggesting that the amino-silane molecules partially undergo protonation during the wet-chemical modification process. Figure 7 shows representative XPS data of the S2s region, where four components are needed to achieve a suitable fit. The peaks at 227 and 228.2 eV correspond to carbon-bonded thiol groups, and can be attributed to the mercaptosilane anchored molecules. The other two peaks at around 228.3 and 229.2 eV are components characteristic of the S–S bond, indicating the formation of intermolecular cross-linking between neighboring silane molecules.

Lastly, the chemistry of the surfaces of differentially modified nanotubes was exploited for practical applications, exploiting the NTs as nanocarriers or nanoextractors which can extract and transfer molecules from one phase to another. Silicon nanotubes with hydrophobic octadecylsilane-modified outer surfaces and with hydrophilic positively charged aminosilane-modified interior surfaces were suspended in a suitable organic solvent, for example, methyl-THF. The organic SiNTs suspension was added to an Eppendorf vial containing a solution of the negatively charged fluorophore fluorescein in water, forming a two separate phase system, as shown in Figure 8A. The mixture was gently agitated overnight to increase the interfacial area, and allowed to settle for approximately 15 min. The NTs which possess hydrophobic outer surfaces remain in the upper organic phase, and the water-soluble fluorescein molecules were clearly transferred across the phase boundary into the nonpolar phase solution, as evident in Figure 8B. Note that for a control experiment carried out without the presence of NTs, no changes in the phase system were observed and the fluorescein molecules remain exclusively in the lower phase. These results indicate that the negatively charged fluorescein molecules, which are insoluble in methyl-THF, are extracted from the aqueous phase into the hydrophilic positively charged inner void of the APTES-modified NTs present and soluble in the nonpolar hydrophobic phase. The brighter fluorescence ring in the phase boundary (Figure 8B) is a result of fluorescent silicon nanotubes precipitating in the interface. Separation of the phases and slight shaking of the nanotubes-containing organic phase lead to resuspension of

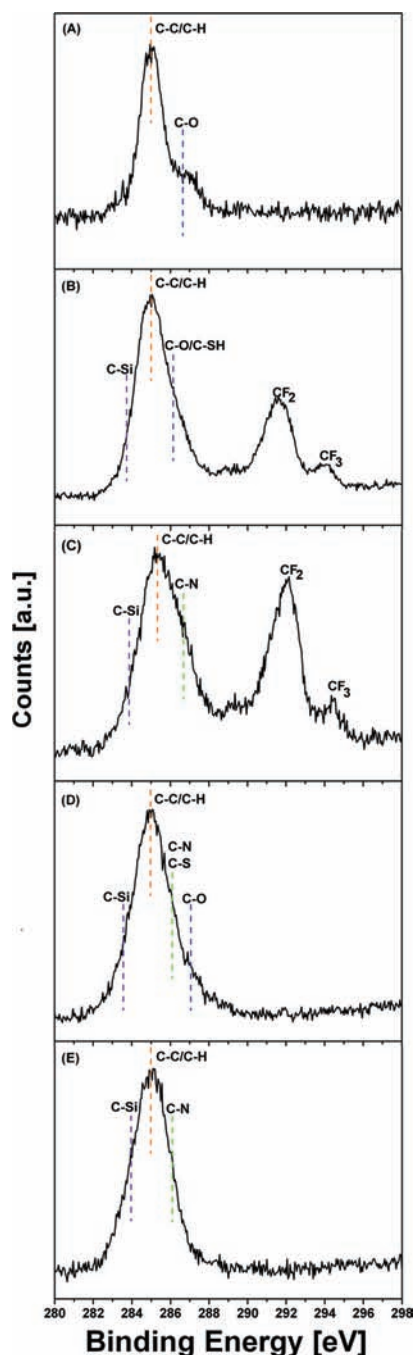


Figure 5. Representative XPS spectra of the C1s region for: (A) reference sample; (B) samples modified with mercaptosilane and fluorosilane molecules (samples 4 and 8) showing CF₂ and CF₃ at 290.9 and 292.69 eV, respectively, C–O or C–SH bond at 286.6 eV (blue dashed line), C–H/C–C bonds at 285 eV (orange dashed line), and C–Si bond at 284 eV (purple dashed line); (C) samples modified with aminosilane and fluorosilane molecules (samples 2 and 7) showing CF₂ and CF₃ at 290.9 and 292.69 eV, respectively, C–N bond at 286 eV (green dashed line), C–H/C–C bonds at 285 eV (orange dashed), and C–Si at 284 eV (purple dashed line); (D) samples modified with aminosilane and mercaptosilane molecules (samples 3 and 6) showing C–N/C–SH bonds at 286 eV (green dashed line), C–H/C–C bonds at 285 eV (orange dashed line), and C–Si at 284 eV (purple dashed line); (E) samples modified with aminosilane and octadecylamine molecules (samples 1 and 5) showing C–H/C–C bonds at 285 eV (orange dashed line) and C–Si bond at 284 eV (purple dashed line).

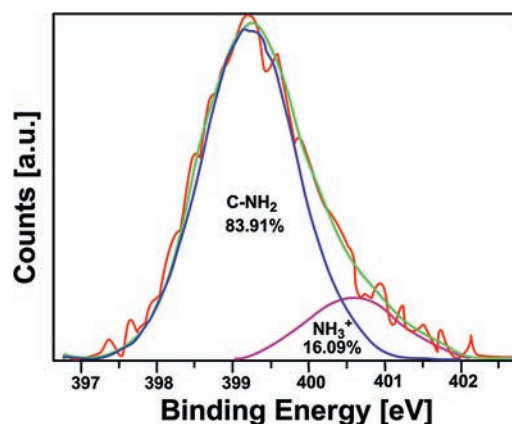


Figure 6. Representative fitted XPS spectrum of N1s region for samples modified with aminosilane molecules showing C–NH₂ (blue) and C–NH₃⁺ (pink) bonds. The red line is the data, the green line is the resulting fit to the spectrum, and the blue and pink lines are the deconvolution.

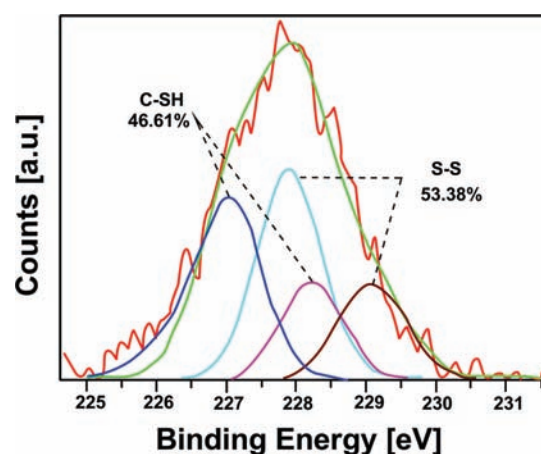


Figure 7. Representative high-resolution XPS spectrum of S2s region for samples modified with mercaptosilane molecules comprises a single doublet from C–SH bond (blue and pink lines) and a single doublet from S–S bonds (pale blue and brown lines).

fluorescent molecules-containing SiNTs. Fluorescence spectra of a solution of modified silicon NTs in methyl-THF, fluorescein in water, and of a sample taken from the upper organic phase (Figure 8B) are shown in Figure 8C. Water-soluble fluorescein (curve a, green) emits green light at 520 nm upon excitation at 488 nm. In contrast to silicon nanotubes sample (curve c, blue) which shows no sign of fluorescence, excitation of the silicon nanotubes sample taken from the upper phase (curve b, red) results in green light emission at 520 nm. The differences in the emission intensities between curve a and curve b can be attributed to the strong scattering of the SiNTs. This two-phase liquid transport/extraction process can be essential for multitude desirable applications such as imaging, concentrating, filtering, and sensing of chemical and biological species.

Furthermore, wall-selective AuNPs-decorated SiNTs can be readily obtained by a similar approach, Figure 9. The decoration of the outer NTs walls can be performed by a simple electroless metal deposition step on the Ge–Si core–shell nanowires prior the removal of the Ge cores. Figure 9 (top) shows a representative TEM image of the Au nanoparticles deposited on the SiNTs. After

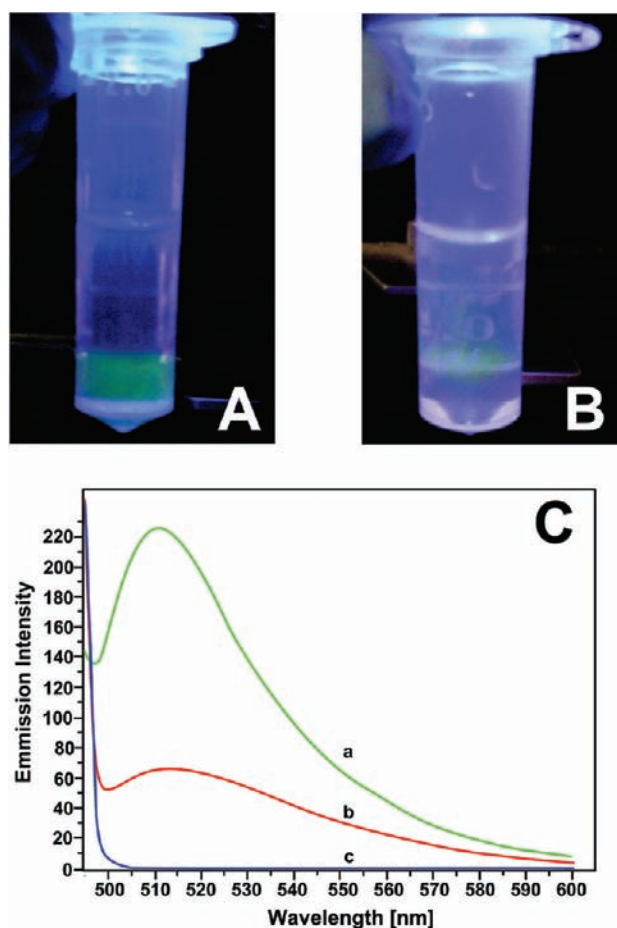


Figure 8. Photographs of Eppendorf vials containing fluorescein in water (lower phase) and solution of modified silicon NTs with hydrophobic octadecylsilane (C18) on the outer surface and aminosilane on the inner surface and methyl-THF (upper phase) under UV light excitation before (A) and after 4 h agitation (B). (C) Photoluminescence (PL) spectra of: (curve a) fluorescein in water, (curve b) modified SiNTs–fluorescein complex in methyl-THF, (curve c) modified silicon NTs in methyl-THF before fluorescein insertion.

the formation of the nanoparticles, the Ge cores are chemically removed leading to outer wall-decorated nanotubes. The density as well as the size of the nanoparticles synthesized can be readily modulated by controlling the electroless deposition conditions. The selective decoration of the inner-walls can be accomplished by initially protecting the outer wall of the nanotubes with an appropriate molecular layer, fluorosilane, which blocks the outer SiNTs walls during the AuNPS decoration step. Then, the Ge cores are removed and the electroless metal deposition of nanoparticles is finally performed. This leads to SiNTs with their inner walls selectively decorated with nanoparticles. Figure 9 (bottom) shows representative TEM images of the SiNTs having their inner walls modified with Au nanoparticles. By exploiting this simple strategy, we can obtain nanotubes selectively decorated with NPs of different metals and semiconductors. Additionally, SiNTs with a combination of metal and/or semiconducting nanoparticles in the inner and outer walls can be synthesized.

To summarize, we developed a method to selectively and differentially modify the inner and outer surfaces of semiconductor silicon nanotubes with various silane molecule derivatives containing

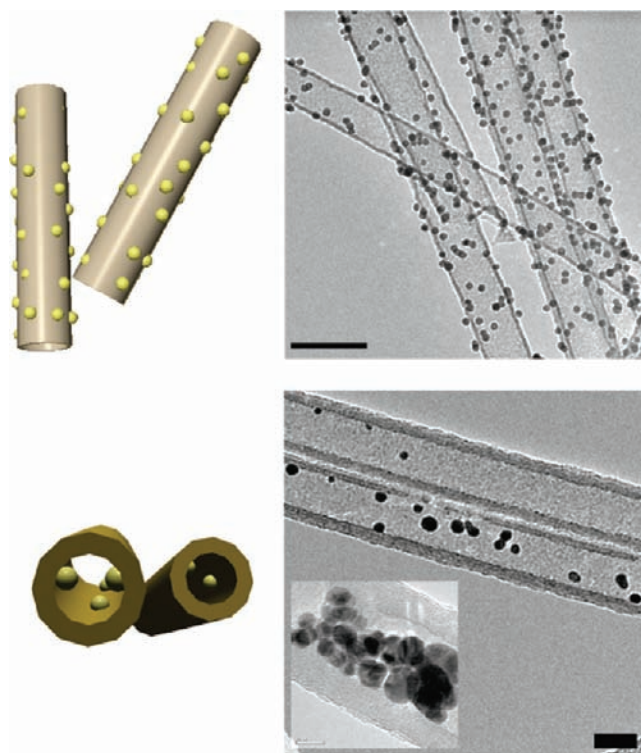


Figure 9. Representative TEM images of (top) outer-wall AuNPs-decorated SiNTs and (bottom) inner-wall AuNPs-decorated SiNTs. Inset: TEM image of SiNTs densely decorated in their inner wall.

different functional groups without affecting their surface integrity. A remarkably broad spectrum of orthogonally modified SiNTs samples can be obtained using this route. SiNTs dispersed in organic solvents with hydrophilic and charge-controlled internal voids, as well as hydrophilic water-dispersed NTs with very hydrophobic internal voids, are readily synthesized. The surface chemistry of the silanized silicon nanotubes has been systematically studied utilizing XPS analysis. Our results reveal that post-treated SiNTs exhibit significant chemical changes after the first and the second modification steps. The ability to selectively control the chemical properties of both the inner and outer surfaces of the nanotubes, and subsequently the different types of chemical media in which the SiNTs can be dispersed, might open up exciting opportunities for the applications of SiNTs, as exemplified in this work by a simple two-phase extraction process. Additionally, the inner and outer walls of the SiNTs can be chemically altered beyond the selective formation of molecular layers, as exemplified by the selective decoration of the NTs walls with metal nanoparticles, or the combination of molecular layers and nanoparticles decoration. These NP-decorated NTs can be further used in many future applications, such as selective catalysis, sensing nanochannel devices and nanofiltering elements. Moreover, the wall-modified SiNTs can be used as a chemical anchoring base for the further modification of biomolecules selectively in the outer and/or inner surfaces of the NTs.

■ ASSOCIATED CONTENT

S Supporting Information. Additional figures as mentioned in the text and complete ref 46. This material is available free of charge via the Internet at <http://pubs.acs.org>.

AUTHOR INFORMATION

Corresponding Author

fernando@post.tau.ac.il

ACKNOWLEDGMENT

This work was in part financially supported by the Legacy Fund-Israel Science Foundation (ISF) and the German-Israel Foundation (GIF). We thank Dr. Larisa Burstein for the performance of XPS measurements and their analysis.

REFERENCES

- (1) Rapoport, L.; Fleischer, N.; Tenne, R. *J. Mater. Chem.* **2005**, *15*, 1782–1788.
- (2) Tenne, R. *Prog. Inorg. Chem.* **2001**, *50*, 269–315.
- (3) Tenne, R.; Zettle, A. K. *Carbon Nanotubes* **2001**, *80*, 81–112.
- (4) Patzke, G. R.; Krumeich, F.; Nesper, R. *Angew. Chem., Int. Ed.* **2002**, *41*, 2446–2461.
- (5) Martin, C. R. *Science* **1994**, *266*, 1961–1966.
- (6) Goldberger, J.; He, R.; Zhang, Y.; Lee, S. W.; Yan, H.; Choi, H. J.; Yang, P. D. *Nature* **2003**, *422*, 599–602.
- (7) Goldberger, J.; Fan, R.; Yang, P. D. *Acc. Chem. Res.* **2006**, *39*, 239–248.
- (8) Sha, J.; Niu, J.; Ma, X.; Xu, J.; Zhang, X.; Yang, Q.; Yang, D. *Adv. Mater.* **2002**, *14*, 1219–1221.
- (9) Schmidt, O. G.; Eberl, K. *Nature* **2001**, *410*, 168.
- (10) Jeong, S. Y.; Kim, J. Y.; Yang, H. D.; Yoon, B. N.; Choi, S.-H.; Kang, H. K.; Yang, C. W.; Lee, Y. H. *Adv. Mater.* **2003**, *15*, 1172–1176.
- (11) Chen, Y. W.; Tang, Y. H.; Pei, L. Z.; Guo, C. *Adv. Mater.* **2005**, *17*, 564–567.
- (12) Tang, Y. H.; Pei, L. Z.; Chen, Y. M.; Guo, C. *Phys. Rev. Lett.* **2005**, *95*, 116102.
- (13) De Crescenzi, M.; Castrucci, P.; Scarcelli, M.; Diociauti, M.; Chaudhari, P. S.; Balasubramanian, C.; Bhave, T. M.; Bhorkar, S. V. *Appl. Phys. Lett.* **2005**, *86*, 231901.
- (14) Xie, M.; Wang, J. S.; Fan, Z. Y.; Lu, J. G.; Yap, Y. K. *Nanotechnol.* **2008**, *19*, 1–4.
- (15) De Heer, W. A.; Bonard, J.-M.; Fauth, K.; Chatelain, A.; Forro, L.; Ugarte, D. *Adv. Mater.* **1997**, *9*, 87.
- (16) Ajayan, P. M. *Chem. Rev.* **1999**, *99*, 1787.
- (17) Baughman, R. H.; Changxing, C.; Zakhidov, A. A.; Iqbal, Z.; Barisci, J. N.; Spinks, B. M.; Wallace, G. G.; Mazzoldi, A.; De Rossi, D.; Rinzler, A. G.; Jaschinski, O.; Roth, S.; Kertesz, M. *Science* **1999**, *284*, 1340.
- (18) Sakata, T.; Kamahori, M.; Miyahara, Y. *Mater. Sci. Eng., C* **2004**, *24*, 827.
- (19) Roy, S.; Vedala, H.; Choi, W. *Nanotechnology* **2006**, *17*, S14.
- (20) Spence, M. M.; Rubin, S. M.; Dimitrov, I. E.; Ruiz, E. J.; Wemmer, D. E.; Pines, A.; Yao, S. Q.; Tian, F.; Schultz, P. G. *Proc. Natl. Acad. Sci. U.S.A.* **2001**, *98*, 10654.
- (21) Tani, K.; Ito, H.; Otno, Y.; Kishimoto, S.; Okochi, M.; Honda, H.; Mizutani, T. *J. Appl. Phys.* **2006**, *45*, 5481.
- (22) Goldberger, J.; Fan, R.; Yang, P. *Acc. Chem. Res.* **2006**, *39*, 239.
- (23) Mitchell, D. T.; Lee, S. B.; Trofin, L.; Li, N.; Nevanen, T. K.; Soderlund, H.; Martin, C. R. *J. Am. Chem. Soc.* **2002**, *124*, 11864.
- (24) Bahr, L. L.; Tour, J. M. *Chem. Mater.* **2001**, *13*, 3823.
- (25) Dyke, C. A.; Tour, J. M. *Nano Lett.* **2003**, *3*, 1215.
- (26) Strano, M. S.; Dyke, C. A.; Uesery, M. L.; Barone, P. W.; Allen, M. J.; Shan, H. W.; Kittrell, C.; Hauge, R. H.; Tour, J. M.; Smalley, R. E. *Science* **2003**, *301*, 1519.
- (27) Strano, M. S.; Huffman, C. B.; Moore, V. C.; O'Connell, M. J.; Haroz, E. H.; Hubbard, J.; Miller, M.; Rialon, K.; Kittrell, C.; Ramesh, S.; Hauge, R. H.; Smalley, R. E. *J. Phys. Chem. B* **2003**, *107*, 6979.
- (28) Hu, H.; Zhao, B.; Hamon, M. A.; Kamaras, K.; Itkis, M. E.; Haddon, R. C. *J. Am. Chem. Soc.* **2003**, *125*, 14893.
- (29) Holzinger, M.; Abraham, J.; Whelan, P.; Graupner, R.; Ley, L.; Hennrich, F.; Kappes, M.; Hirsch, A. *J. Am. Chem. Soc.* **2003**, *125*, 8566.
- (30) Liang, F.; Sadana, A. K.; Peera, A.; Chattopahyay, J.; Gu, Z.; Hauge, R. H.; Billups, W. E. *Nano Lett.* **2004**, *4*, 1257.
- (31) Chen, R. W.; Eklund, P. C.; Colbert, D. T.; Smalley, R. E.; Haddon, R. C. *J. Phys. Chem. B* **2001**, *105*, 2525.
- (32) Chen, J.; Hamon, M. A.; Hu, H.; Chen, Y.; Rao, A. M.; Eklund, P. C.; Haddon, R. C. *Science* **1998**, *282*, 95.
- (33) Mickelson, E. T.; Huffman, C. B.; Rinzler, A. G.; Smalley, R. E.; Hauge, R. H.; Margrave, J. L. *Chem. Phys. Lett.* **1998**, *296*, 188.
- (34) Chen, Q.; Dai, L.; Gao, M.; Huang, S.; Mau, A. *J. Phys. Chem. B* **2001**, *105*, 618.
- (35) Vast, L.; Philippin, G.; Destree, A.; Moreau, N.; Fonseca, A.; Nagy, J. B.; Delhalle, J.; Mekhalif, Z. *Nanotechnology* **2004**, *15*, 781.
- (36) Hamon, M. A.; Chen, J.; Hu, H.; Chen, Y.; Itkis, M. E.; Rao, A. M.; Eklund, P. C.; Haddon, R. C. *Adv. Mater.* **1999**, *11*, 834.
- (37) Bachilo, S. M.; Strano, M. S.; Kittrell, C.; Hauge, R. H.; Smalley, R. E.; Weisman, R. B. *Science* **2002**, *298*, 2361.
- (38) Ramesh, S.; Ericson, L. M.; Davis, V. A.; Saini, R. K.; Kittrell, C.; Pasquall, M.; Billups, W. E.; Adams, W. W.; Hauge, R. H.; Smalley, R. E. *J. Phys. Chem. B* **2004**, *108*, 8798.
- (39) Whitby, M.; Cagnon, L.; Thanou, M.; Quirke, N. *Nano Lett.* **2008**, *8*, 2632.
- (40) Whitby, M.; Quirke, N. *Nature Nanotechnol.* **2007**, *2*, 87.
- (41) Liu, Y.; Wang, Q.; Zhang, L. *J. Chem. Phys.* **2005**, *123*, 234701.
- (42) Dong, L.; Tao, X.; Hamdi, M.; Zhang, Li.; Zhang, X.; Ferreira, A.; Nelson, B. J. *Nano Lett.* **2009**, *9*, 210.
- (43) Katz, E.; Willner, I. *ChemPhysChem* **2004**, *5*, 1084.
- (44) Tang, C.; Bado, Y.; Huang, Y.; Yue, S.; Gu, C.; Xu, F.; Golberg, D. *J. Am. Chem. Soc.* **2005**, *127*, 6552.
- (45) Saini, R. K.; Chiang, L. W.; Peng, H.; Smalley, R. E.; Billups, W. E.; Hauge, R. H.; Margrave, J. L. *J. Am. Chem. Soc.* **2003**, *125*, 3617.
- (46) Campidelli, S.; et al. *J. Am. Chem. Soc.* **2008**, *130*, 11503.
- (47) Wang, W.; Bando, Y.; Zhi, C.; Fu, W.; Wang, E.; Golberg, D. *J. Am. Chem. Soc.* **2008**, *130*, 8144.
- (48) Li, D.; McCann, J. T.; Xia, Y. *Small* **2005**, *1*, 83.
- (49) Park, M.-H.; Kim, M. G.; Joo, J.; Kim, K.; Kim, J.; Ahn, S.; Cui, Y.; Cho, J. *Nano Lett.* **2009**, *9*, 3844.
- (50) Lan, J.; Cheng, D.; Cao, D.; Wang, W. *J. Phys. Chem. C* **2008**, *112*, 5598.
- (51) Bai, J.; Zeng, X. C.; Tananka, H.; Zeng, J. Y. *Proc. Natl. Acad. Sci. U.S.A.* **2004**, *101*, 2664.
- (52) Ben-Ishai, M.; Patolsky, F. *J. Am. Chem. Soc.* **2009**, *131*, 3679.
- (53) Ben-Ishai, M.; Patolsky, F. *Angew. Chem. Int. Ed.* **2009**, *46*, 8699–8702.
- (54) Ben-Ishai, M.; Patolsky, F. *Advanced Materials* **2010**, *8*, 902–906.
- (55) Wanger, C. D.; Riggs, W. M.; Davis, L. E.; Moulder, J. F.; Muilenberg, G. E. In *Handbook of X-ray Photoelectron Spectroscopy*; Physical Electronics: Eden Prairie, MN, 1979.
- (56) Graf, N.; Yegen, E.; Gross, T.; Lippitz, A.; Weigel, W.; Krakert, S.; Terfort, A.; Unger, Wolfgang, E. S. *Surf. Sci.* **2009**, *603*, 2849.
- (57) Sprenger, D.; Anderson, O. *Fresenius' J. Anal. Chem.* **1991**, *341*, 116.
- (58) Pevzner, A.; Engel, Y.; Elnathan, R.; Ducobni, T.; Ben-Ishai, M.; Reddy, K.; Shpaisman, N.; Tsukernik, A.; Oksman, M.; Patolsky, F. *Nano Lett.* **2010**, *10*, 1202–1208.